Correlation of entropy with optimal pinning density for the control of spatiotemporal chaos

Alex Greilich[1] and Mario Markus[2]

[1,2] *Max-Planck-Institut fuer molekulare Physiologie, Postfach 500247, D-44202 Dortmund, GERMANY*
E-mails: alex.greilich@mpi-dortmund.mpg.de markus@mpi-dortmund.mpg.de

(Received 16 November 2002)

We consider three systems that are spatially one-dimensional and are discretized in space and time: i) cellular automata proposed by Wolfram; ii) a system that has been used as a prototype for coupled map lattices; and iii) a coupled map lattice that provides a simple description of earthquakes. Chaotic modes of these systems can be made periodic by external forcing at points equidistant in space ("pinnings"). The minimum distance between these points - corresponding to the optimal pinning density - is correlated to the spatial measure entropy S via a single-valued relationship. In other words, determination of S straightforwardly yields optimal spacings for a forcing that turns unpredictable into predictable behaviour.

Key words: spatiotemporal chaos, turbulence, chaos control, cellular automata, coupled map lattices

PACS numbers: 05.45Ra, 05.45Gg; 87.17.Aa

1 Introduction

Control of chaos in low-dimensional systems has been intensively investigated for more than a decade [1, 2, 3, 4, 5]. Less attention has been paid as yet to spatially extended systems. In the latter, the main challenge has been to control the whole system by externally regulating a finite subset of the totality of degrees of freedom. One way to tackle this is to control single, usually equidistant points in space ("pinnings"). Control with this method has been accomplished in coupled map lattices [6, 7, 8, 9], in the complex Ginzburg-Landau equation [10, 11] and in partial differential equations [12]; applications involving neural tissue have been reported [13, 14, 15].

Our work addresses the optimization of the process by determining the minimum density (maximum distance) of pinnings necessary for successful control. Our goal was to correlate this density to a quantity that can be determined in the absence of pinnings; this quantity can then be used to determine the optimal density in each particular case. As we shall report here, we found that the spatial measure entropy is a quantity that fulfills this goal.

As first steps in our line of work, we use spatially one-dimensional cellular automata (CAs; Section 3) and coupled map lattices (CMLs; Section 4). In Section 5 we investigate a CML that describes seismological processes. CAs and CMLs [16, 17] have proven to be useful tools for the simulation in a large number of areas. Examples are: fluid dynamics [18], ferromagnetism [16], immunology, brain paternization, ecology and growth of fungi and bacterial colonies [19], growth of leaf veins and vascular networks [20], cellular calcium waves [21], excitable media [22], pigmentation of skins and furs [23], pattern formation on the shells of molluscs [24], and seismology [25, 26, 27]. Both time and space are discrete in CAs and CMLs; phase variables are discrete in CAs and continuous in CMLs. Iterative rules in CAs and CMLs are set so as to describe the essential features of a system. Calculations are usually faster and easier to programm than those with partial differential equations. The price one has to pay for this advantage is a loss of precision of the results. Nevertheless, CAs and CMLs can render useful qualitative descriptions of nature, pointing to essential properties of the systems [26]; surpris-

ingly, even quantitative comparisons of CA simulations with experiments have been reported [21].

2 General definitions and methods

One-dimensional systems consisting of cells $i = 1, 2, ..., L$ are considered at times $n = 1, 2, ..., T$. We assume periodic boundary conditions for any phase variable $x_n(i)$, i.e. $x_n(i + L) = x_n(i)$. $x_{n+1}(i)$ depends only on $x_n(i)$ and on the values of the r neighbors on each side of the cell i: $x_n(i-r), \ldots, x_n(i+r)$. All calculations are performed starting with values of $x_n(i)$ randomly distributed in space.

The spatial measure entropy S [28] is defined as

$$S = -\frac{1}{X}\sum_{j=1}^{k^X} p_j \log_k p_j, \qquad (1)$$

considering cell blocks of spatial length X and k states in each cell. The number of possible sequences of states in a block is k^X; p_j is the probability of the sequence of states j. S is determined in the absence of pinnings by considering all blocks obtained between the time step $n = 500$ and T. (The first 500 steps are skipped to allow transients to die away).

In a random distribution all the k^X sequences are equally probable and S is maximum. In our work we were lead by the intuitive conjecture that randomness requires the highest density of pinnings, while a lower S indicates a more ordered system and thus requires less dense control.

In all our investigations we determine a distance d_{crit} of pinnings as follows. We calculate until $n = T$, first with a pinning distance $d = 1$, then $d = 2$, then $d = 3$, and so on. d_{crit} fulfills the condition that the system becomes periodic everywhere for $d < d_{crit}$, but remains chaotic somewhere in space for $d = d_{crit}$.

3 Control of chaos in cellular automata

We consider automata proposed by S. Wolfram [16,28], which have been used as prototypes because they display general properties of CAs. We set $k = 2, r = 2, L = 2000$ and assume totalistic rules, i.e. $x_n(i+1)$ depends only on the sum σ over the neighbors $x_n(m)$, $m = i-2, i-1, i, i+1, i+2$.

The binary output $f(\sigma)$ of the rules is coded by

$$C = \sum_{\sigma=0}^{5} 2^\sigma f(\sigma). \qquad (2)$$

It had been shown that the 16 CAs coded by C=2,6,10,12,14,18,22,26,28,30,34,38,42,44,46 and 50 yield chaotic patterns. Each of the 16 points in Figures 1a or 1b corresponds to one of these chaotic automata. Figure 1a is obtained by forcing the pinning sites to the temporally periodic string 001100110011... One observes in this figure only slight scattering of the points around a single-valued relation between d_{crit} and S. The following function can be fitted to these points:

$$d_{crit} = \alpha e^{\beta x} \qquad (3)$$

with $\alpha = 468.6$ and $\beta = -5.15$. Setting the temporal string to 000111000111000111... also yields a single-valued relation; it can be fitted with $\alpha = 259.6$ and $\beta = -5.70$. In contrast, forcing with 01010101... renders scattering in the order of the mean, as shown in Figure 1b, so that a single-valued approximation is not reasonable. This example shows that one has to be careful when choosing a control procedure. In other words, the first step in the method proposed in this paper is to find a procedure that yields single-valuedness.

Figure 1 was obtained with an automaton length $L = 2000$, block size $X = 6$ and total running time $T = 5000$. A change in L, X or T does not change the occurrence or non-occurrence of single-valuedness. However, a decrease of X shifts the $d_{crit}(S)$-curve to the right, while a decrease of T shifts this curve downwards. The latter result is explained by long-lived chaotic transients, which require denser pinning if the total time is shorter. The

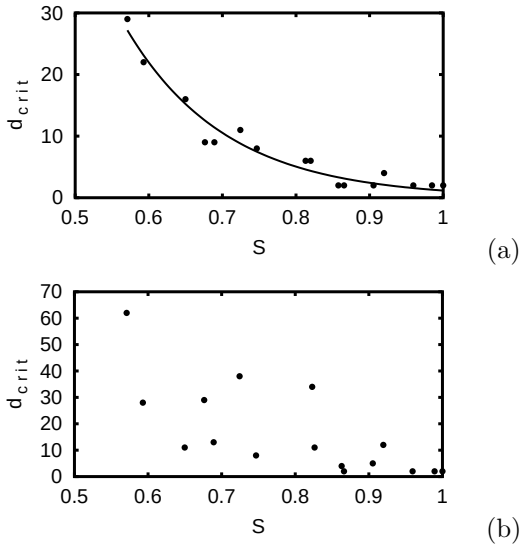

FIG. 1. Maximum distance d_{crit} of pinning sites versus the spatial measure entropy S for binary automata proposed by Wolfram. Each point on each figure corresponds to one of the 16 known chaotic totalistic automata. Forcing at pinning sites: 001100110011...(a) and 01010101...(b)

shifts of the curves due to changes in X and T can be quantified by changes in α and β. Examples with the string 0011001100... are: $\alpha = 213.0$ and $\beta = -4.45$ for $X = 12$ and $T = 5000$; $\alpha = 602.5$ and $\beta = -5.75$ for $X = 6$ and $T = 2000$.

Figure 2 illustrates the effect of increasing d at fixed running time T and fixed rule code C. We set $L = 200$. We obtain $d_{crit} = 6$. Note that for $d = 7$ the behaviour remains chaotic for n close to T (lower left and right of Figure 2d). For $d < d_{crit}$ (Figures 2b and 2c), the control procedure induces complex periodical structures having a width between 6 and 20 cells.

4 Control of coupled map lattices

We carry out investigations with the following model, which has been used as a prototype for coupled map lattices [29-33]:

$$x_{n+1}(i) = G(\varepsilon, i, i-1, i+1), \tag{4}$$

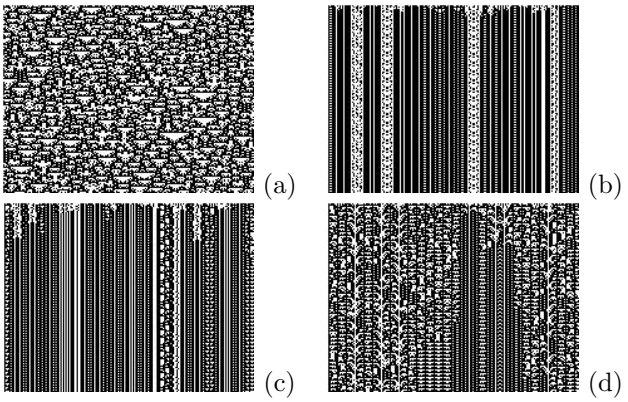

FIG. 2. Patterns in space (horizontally) and time (vertically downwards) for Wolfram's totalistic rule 26. Forcing at pinning sites: 0011001100... a) No pinnings; chaotic behaviour. b) Chaos control with pinning site distance d=3. c) Chaos control with d=4. d) Failure of chaos control with d=7

where

$$G(\varepsilon, i, i-1, i+1) = (1-\varepsilon) f\left[x_n(i)\right] + \frac{\varepsilon}{2}\left\{f\left[x_n(i-1)\right] + f\left[x_n(i+1)\right]\right\}. \tag{5}$$

For $f(x)$ we take the logistic map

$$f(x) = ax(1-x). \tag{6}$$

We set $a = 4$, so that this map is chaotic. To control the system, we set pinnings as in [6]:

$$x_{n+1}(i) = G(\varepsilon, i, i-1, i+1) + \sum_{k=0}^{L/d} \delta(i-dk-1) g_n, \tag{7}$$

where d is the pinning distance. $\delta(j) = 1$ for $j = 0$ and $\delta(j) = 0$ otherwise. g_n is given by

$$g_n = (1-\varepsilon)F(i) + \frac{\varepsilon}{2}F(i-1) + \frac{\varepsilon}{2}F(i+1), \tag{8}$$

where

$$F(j) = p_n(j) x_n(j) [x_n(j) - \overline{x}_n(j)]. \tag{9}$$

ε describes the coupling between neighboring cells. $p_n(j)$ is the feedback strength added to the jth site. We set $p_n(j) = p = const.$ $\overline{x}_n(j)$ is a reference state towards which the system is driven. Here:

$$\overline{x}_n(j) = 1 - \frac{1}{a}, \tag{10}$$

which is a fixed point of the logistic map given by Equation (6). Note that the $x_n(i)$ are points in the interval [0,1]. S is determined by dividing the unit interval in 10 segments of length 0.1 each. One state is assigned to each of these segments; thus $k = 10$.

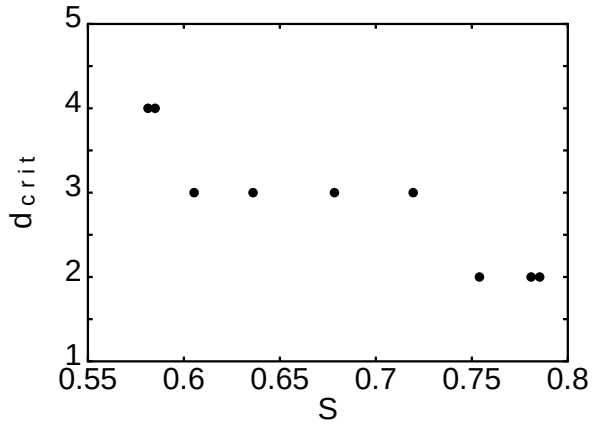

FIG. 3. Maximum distance d_{crit} of pinning sites versus spatial measure entropy S for the coupled map lattice described in Section 4

In Figure 3 we show the dependence of d_{crit} on the entropy S. We vary the entropy by varying $\varepsilon \in [0, 0.8]$ in steps equal to $\Delta\varepsilon = 0.1$. Control is not necessarily achieved by obtaining the constant reference state, but also by periodic oscillations around this state. As in the case of Wolfram's automata (Figure 1a), we obtain in Figure 3 a single-valued relation. This figure is obtained for $p = 2.4, L = 600, X = 6$ and $T = 5000$. Changes of L have no influence on the results. Changes of X and T preserve the single-valuedness, but shift the points in Figure 3 analogously to the corresponding shifts of Figure 1a (see Section 3). The space-time patterns are similar to those in Figure 2.

5 A seismological application

Figure 4 shows the geometry of a one-dimensional stick-slip model, which has been used for a simplified description of earthquakes. [25-27,34,35]. The continental plate is assumed to be composed of identical blocks. These blocks are connected to their two neighbors by springs - to simulate plate elasticity - and are lying or slipping over the rigid oceanic plate. It is assumed that, due to the movement of the continental plate, a constant amount of energy is transferred to each block per unit time. Slipping of a block occurs when its total potential energy exceeds a given threshold. This energy is then partially dissipated and partially distributed equally among the two neighbors. It should be noticed that this model is operating in two different time-scales corresponding to two different processes in nature; the increase of energy to each block takes up a long time (resting state in the range of years or more), while the slipping of the blocks (earthquakes) occurs in a short period (seconds or minutes). In CMLs, however, the totality of each resting state is simulated in one single time step.

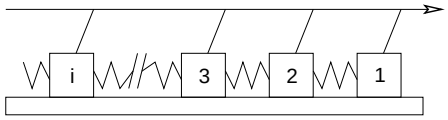

FIG. 4. Scheme explaining the seismological stick-slip model

The phase variable $x_n(i)$ is, in this model, the potential energy of block i at time n. We assume that, owing to the plate movement, the energy is increased by 1 for all blocks after all blocks have come to rest. $x_n(i) = 0$ means that there is no tension on the block; $x_n(i) < 2$ means that there is tension but the block doesn't slip. A block slips if $x_n(i) \geq 2$, $x_n(i)$ becoming zero after slipping and delivering the energy $(x_n(i)-D)/2$ to each neighbor; D is the dissipated energy.

Analyzing only the Poincaré section defined by resting time steps, i.e. times steps in which $x_n(i) < 2$ for all i, it has been shown that variation of the energy dissipation D causes transitions between chaos, undecidability (class 4 behaviour [27,28]) and periodicity; these three possibilities are illustrated in Figure 5. The $x_n(i)$ are updated as follows:

$$x_n^+(i) = \begin{cases} [x_n(i+1) - D]/2 & if \quad x_n(i+1) \geq 2 \\ 0 & else \end{cases} \tag{11}$$

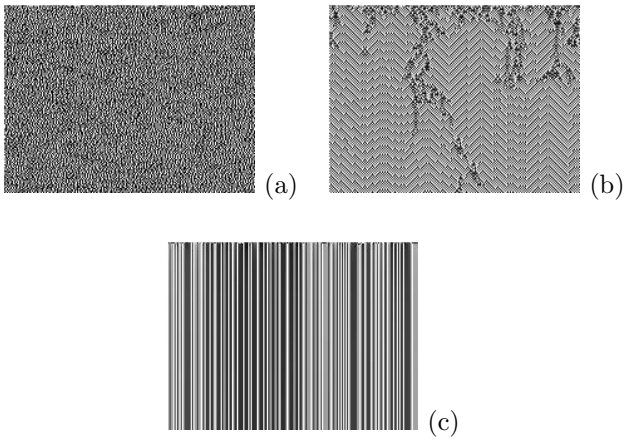

FIG. 5. Patterns in space (horizontally) and time (vertically downwards) resulting from the seismological model without pinnings. Only times without earthquakes are shown. Grey levels correspond to the potential energy of the resting blocks. a) Energy dissipation $D = 0.1$, leading to chaos. b) $D = 0.7$, leading to so-called undecidability. c) $D = 1$, leading to periodicity.

$$x_n^-(i) = \begin{cases} [x_n(i-1) - D]/2 & if \quad x_n(i-1) \geq 2 \\ 0 & else \end{cases} \tag{12}$$

$$x_n^0(i) = \begin{cases} x_n(i) & if \quad x_n(i) < 2 \\ 0 & else \end{cases} \tag{13}$$

Here, $x_n^+(i)$ is the contribution to the potential energy from the right, $x_n^-(i)$ that from the left, and $x_n^o(i)$ the contribution of the considered block itself. These three contributions are added to obtain the new potential energy of block n:

$$x_{n+1}(i) = x_n^+(i) + x_n^-(i) + x_n^o(i). \tag{14}$$

Note that two versions based on this model have been reported. In one of them a binary discretization of $x_n(i)$ is performed each time all blocks come to rest, the intention being a comparison of the dynamics with binary automata [26,27]. In the other version no discretizations are done [25], i.e. the model is defined solely by the rules given here above. This latter version, which is a CML and which is used in the present work, yields the well-known Gutenberg-Richter statistics observed in nature, i.e. $\log N = a - bM$; the magnitude M is $\log m$, where m is the seismic moment; N is the the number of earthquakes with a magnitude larger than M [25,26].

The entropy is determined by considering only the resting time steps ($x_n(i) < 2$ for all i) and dividing the potential energy interval [0,2[in 20 segments of length 0.1. One state is assigned to each of these segments, i.e. $k = 20$. A (nearly) single-valued relation between d_{crit} and S (Figure 6) is achieved by controlling as follows. For all values of n at which the blocks slip, i.e. during earthquakes and not during resting time steps, the potential on all pinning sites is set to the average of $x_n(i)$ over all i. We set $L = 600, X = 6, T = 5000$. S is changed by changing the energy dissipation $D \in [0.1, 1.4]$, but considering only chaotic processes, such as that in Figure 5a. Intuitively one could assume that the averaging procedure would lead to homogeneity; however, in most cases this control procedure leads to periodicity.

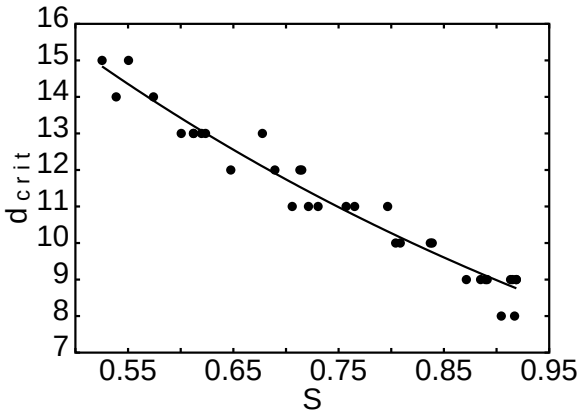

FIG. 6. Maximum distance of pinning sites d_{crit} versus the spatial measure entropy S for the seismological model described in Section 5.

As in the case of Figure 1a, we can fit here the function given by Equation (3) with $\alpha = 602.6$ and $\beta = -5.75$. Changes of L had no effect. Changes in X and T cause shifts that are analogous to the corresponding shifts of the points on Figure 1a, as discussed in Section 3, or of the points on Figure 3 (see Section 4).

6 Conclusion

For the three investigated systems (a general CA, a general CML, and a CML applied to seismology) we find a control procedure such that d_{crit} versus S is nearly single-valued. Without necessarily restricting oneself to these examples, one can state: an unpredictable system can be made predictable if there exists an external forcing that leads to a single-valued relation between d_{crit} and S; in a particular situation it is then sufficient to determine S and to set the pinning sites accordingly. We must stress, however, that care has to be taken in the choice of the procedure for external forcing, since not all procedures lead to single-valuedness, as exemplified in Figure 1b. It is left to future work to find the conditions that forcing must fulfill to render a single-valued relation between d_{crit} and S. The method presented here could be especially useful for the control of unpredictable phenomena in nature, e.g. in geological processes.

References

[1] E. Ott, C. Grebogi, J.A. Yorke. Phys. Rev. Lett. **64**, 1196-1199 (1990)

[2] W.L. Ditto, S.N. Rauseo, M.L. Spano. Phys. Rev. Lett. **65**, 3211-3214 (1990)

[3] K. Pyragas. Phys. Lett. A **170**, 421-428 (1992)

[4] K. Pyragas. Phys. Rev. Lett. **86**, 2265-2268 (2001)

[5] Complete volume. Int. J. Bifurcation and Chaos **12** no.5, 883-1225 (2002)

[6] H. Gang, Q. Zhilin. Phys. Rev. Lett. **72**, 68-71 (1994)

[7] G. Hu, Z.L. Qu. Phys. Rev. Lett. **72**, 68-71 (1994)

[8] Y. Ohishi, H. Ohashi, M. Akiyama. Jap. J. Appl. Phys. (Part 2) **34**, L1420-L1422 (1995)

[9] R.O. Grigoriev, M.C. Cross, H.G. Schuster. Phys. Rev. Lett. **79**, 2795-2798 (1997)

[10] J.H. Gao, J.H. Xiao, Y.G. Yao, G. Hu. Comm. theor. Phys. **32**, 481-488 (1999)

[11] S. Mizokami, Y. Ohishi, H. Ohashi. Physica A **239**, 227-234 (1997)

[12] G. Hu, K.F. He. Phys. Rev. Lett. **71**, 3794-3797 (1993)

[13] J.E. Moreira, F.W.S. Lima, J.S. Andrade. Phys. Rev. E **52**, R2129-R2132 (1995)

[14] C.G. He, Z.T. Cao. Acta Phys. Sinica **50**, 2103-2107 (2001)

[15] N. Parekh, S. Sinha. Phys. Rev. E **65**, 036227 (2002)

[16] S. Wolfram. *Theory and Applications of Cellular Automata* (World Scientific, Singapore, 1986)

[17] *Cellular Automata and Complex Systems.* Edited by E. Goles and S. Martinez (Kluwer, Dordrecht, 1999)

[18] U. Frisch, R. Hasslacher, Y. Pomeau. Phys. Rev. Lett. **56**, 1505-1508 (1988)

[19] G.B. Ermentrout, L. Edelstein-Keshet. J. theor. Biol. **160**, 97-133 (1993)

[20] M. Markus, D. Boehm, M. Schmick. Math. Biosci. **156**, 191-206 (1999)

[21] J. Lechleiter, S. Girard, E. Peralta, D. Clapham. Science **252**, 123-126 (1991)

[22] M. Markus, B. Hess. Nature **347**, 56-58 (1990)

[23] H. Schepers, M. Markus. Physica A **188**, 337-343 (1992)

[24] I. Kusch, M. Markus. J. theor. Biol. **178**, 333-340 (1996)

[25] M. Markus, H. Emmerich, C. Schaefer, P. Almeida, A. Ribeiro. In: *Fractals and Dynamic Systems in Geosciences.* Edited by J. Kruhl (Wuerz, Winnipeg) pp. 181-196 (1994)

[26] M. Markus, A. Czajka, D. Boehm, T. Hahn, T. Schulte, A. Ribeiro. In: *Cellular Automata in Complex Systems.* Edited by E. Goles and S. Martinez (Kluwer, Dordrecht), pp. 55-105 (1999)

[27] M. Markus, T. Hahn, I. Kusch. Parallel Comp. **23**, 1635-1642 (1997)

[28] S. Wolfram. Physica D **10**, 1-35 (1984)

[29] K. Kaneko. Progr. theor. Phys. **74**, 1033-1044 (1985)

[30] K. Kaneko. Physica D **37**, 60-82 (1989)

[31] J.P.Crutchfield, K. Kaneko. Phys. Rev. Lett. **60**, 2715-2718 (1988)

[32] J.D. Keeler, J.D. Farmer. Physica D **23**, 413-435 (1986)

[33] E.J. Ding, Y.N. Lu. J. Phys. A **25**, 2897-2906 (1992)

[34] P. Bak, C. Tang. J. Geophys. Res. **94**, 15.635-15.637 (1989)

[35] R. Burridge, L. Knopoff. Bull. Sci. Soc. Am. **57**, 341-371 (1967)